Supplementary Information

Characterization of nitrogen species incorporated into graphite using low energy nitrogen ion sputtering

Hisao Kiuchi,[1] Takahiro Kondo,[2] Masataka Sakurai,[2] Donghui Guo,[2] Junji Nakamura,[2]

Hideharu Niwa,[3,4] Jun Miyawaki,[3,4] Maki Kawai,[1]

Masaharu Oshima,[4] and Yoshihisa Harada[3,4,*]

[1] Department of Applied Chemistry, University of Tokyo, 7-3-1 Hongo, Bunkyo-ku,

Tokyo, 113-8656, Japan

[2] Faculty of Pure and Applied Sciences, University of Tsukuba, Japan

[3] The Institute for Solid State Physics (ISSP), University of Tokyo, Japan

[4] Synchrotron Radiation Research Organization, University of Tokyo, Japan

Corresponding author:

*E-mail: harada@issp.u-tokyo.ac.jp

Surface morphology of N-HOPG

We examined the surface morphology of N-HOPG by AFM to identify the difference in surface area among our model HOPG samples. All surfaces of HOPG model samples were flat with no distinct differences, as shown Fig. S1. This implies that nitrogen doping followed by an annealing process did not significantly affect the specific surface areas of the prepared samples.
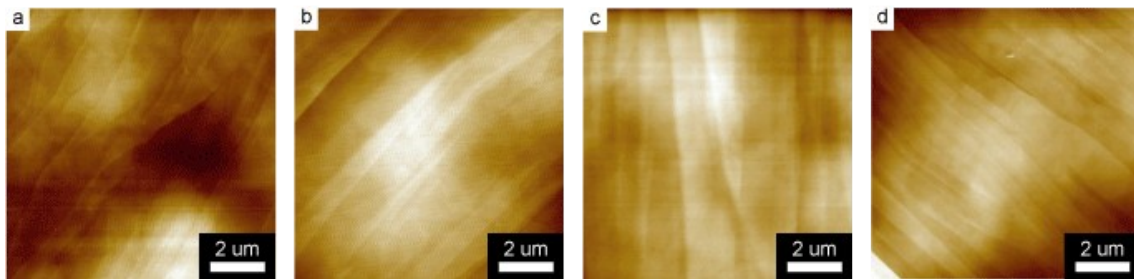

Fig. S1. AFM images of N-HOPG (X = 0.4 (a), 2.3 (b), and 8.4 (c)) and clean HOPG (d).

Depth profile simulation of nitrogen ions doped into HOPG

In order to estimate the depth profile of the nitrogen concentration in HOPG sputtered with N_2^+ ions (Fig. S2), we used the Stopping and Range of Ions in Matter (SRIM) package,[1] a Monte Carlo simulation tool which yields the distribution of implanted ions, vacancies, and sputtered ions, along with surface defects. In this sputtering process, the initial kinetic energy (200 V) was equally distributed among the N_2^+ ions.[2] Ion energy, lattice binding energy,[3] surface binding energy,[4] and displacement energy[4] were set at 100 eV, 3 eV, 7.41 eV, and 35 eV, respectively. In this case, ion energy is the incident energy of a nitrogen atom, and the lattice binding energy is the minimum energy required to remove an atom from its lattice site. In addition, the surface binding energy is the energy required to remove an atom at the target surface, and can be estimated from the heat of sublimation. Finally, the displacement energy is the minimum energy required to knock a target atom from its lattice site.
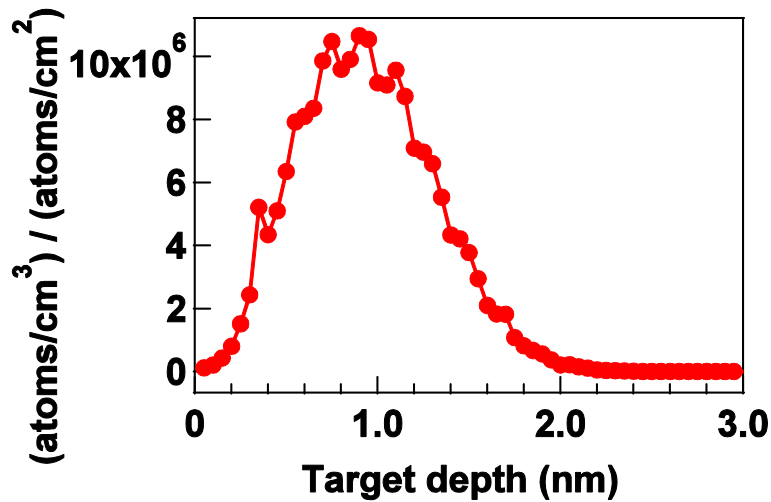

Fig. S2. The simulated depth profile of doped nitrogen ions on HOPG.

Chemical states of nitrogen measured by low energy resolution N 1s XPS

Figure S3 shows the N 1*s* XPS spectra of N-HOPG obtained using a monochromatic Al-Kα source (JPS-9010, JEOL) and an energy resolution of 0.7-0.8 eV. All spectra were normalized according to area intensity. The corresponding high resolution (ΔE = 170 meV) data for N-HOPG with X = 0.4 and 2.3 are shown in Fig. 1. The peak shift to the higher binding energy at approximately 0.8 eV occurred in N-HOPG with X = 0.4, which is consistent with Fig. 1. The relative ratio of the pyridinic N gradually increased from N-HOPG with X = 0.4 to N-HOPG with X = 8.4.
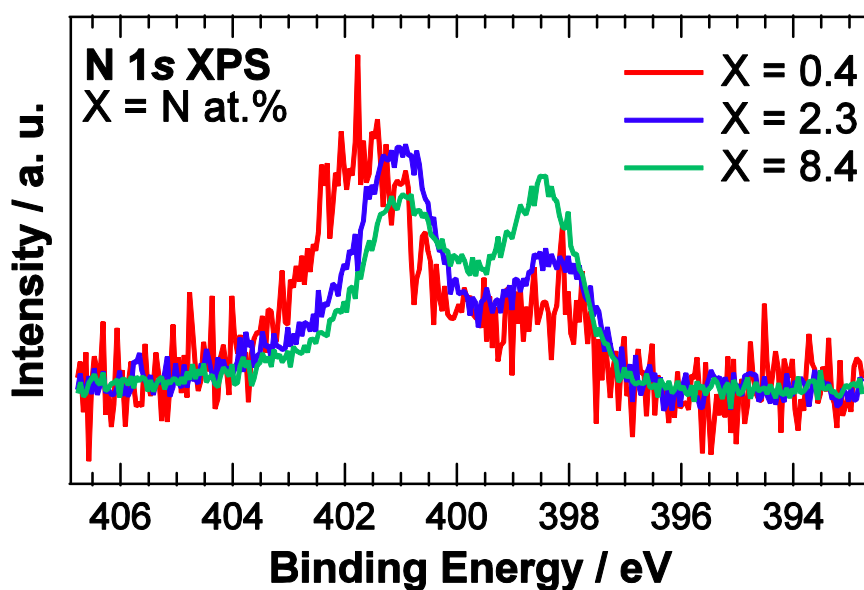

Fig. S3. N 1*s* XPS spectra of N-HOPG (X = 0.4, 2.3, and 8.4).

Chemical states of nitrogen measured by low energy resolution N 1s XPS at low nitrogen content region

Figure S4 shows the N 1s XPS spectra of N-HOPG obtained using a non-monochromatic Al-Kα source (JPS-9010, JEOL) and an energy resolution of 1.1-1.3 eV. The calculated N 1s spectra of Fig.1 with comparable Gaussian parameter of 2.04 eV are also added as references. It is unambiguous that the peak at 401.9 eV is experimentally observed at low nitrogen content. The amount of pyridinic N, graphitic1 N, and graphitic2 N increases in proportion to the total nitrogen content under X = 0.6, however, that of valley N becomes constant over X = 0.9, corresponding to the onset of the amorphization.
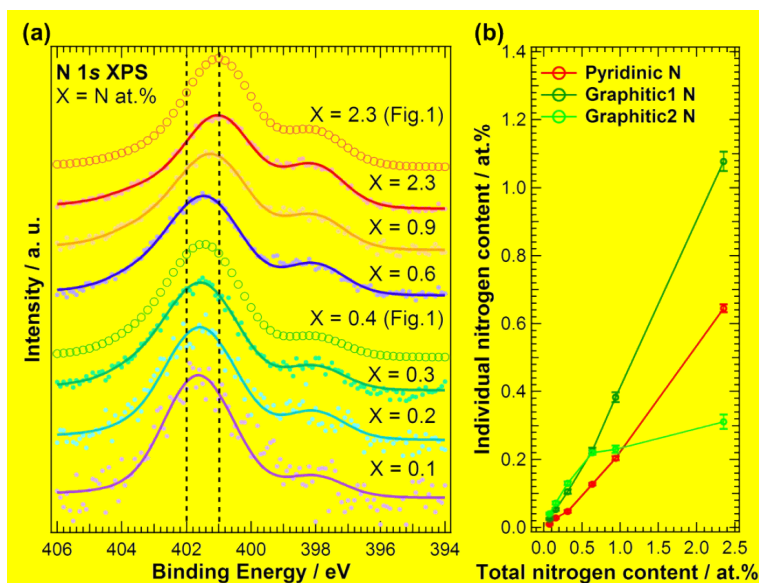

Fig. S4. (a) N 1s XPS spectra of N-HOPG measured with a non-monochromatic Al-Kα source (X = 0.1, 0.2, 0.3, 0.6, 0.9, and 2.3) and the calculated fitting results in Fig.1 (X = 0.4 and 2.3) using comparable Gaussian width of 2.04 eV. Closed circles, solid lines, and open circles represent raw data, fitted data, and calculated fitting results, respectively. (b) The amounts of individual nitrogen components as a function of the total nitrogen content.

Configuration of doped nitrogen in N-HOPG by changing the incident X-ray angles

Figure S5 shows N 1s XAS spectra of N-HOPG. The spectra are normalized using the intensity at 430 eV, taking an average between 390-395 eV as background. The N 1s XAS spectra of N-HOPG with X = 0.4 and 2.3 were obtained at SPring-8 BL27SU, while that of N-HOPG with X = 8.4 was obtained at SPring-8 BL07LSU.[5] Energy resolution was greater than 100 meV for both beam lines. The calculated out-of-plane (θ = 90°) XAS spectrum in Fig. 2 was extracted from the combination of data taken at different X-ray incident angles. The intensity of horizontal and vertical electronic states in each spectrum is proportional to the values of $\sin^2\theta$ and $\cos^2\theta$, respectively.[6]
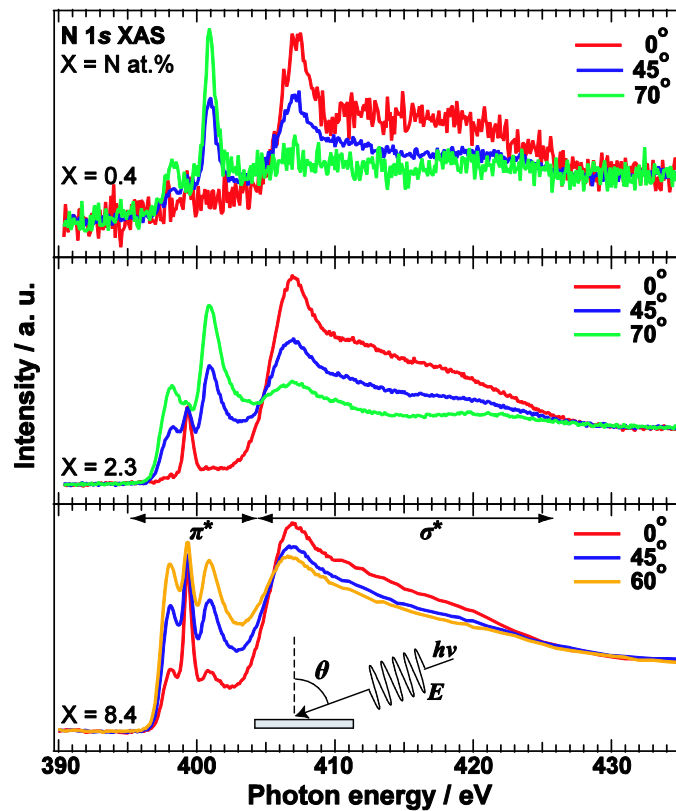

Fig. S5. N 1s XAS spectra of N-HOPG (X = 0.4, 2.3, and 8.4). Red, blue, orange, and green lines correspond to the spectra obtained with incident angles θ = 0°, 45°, 60°, and 70°.

Surface carbon morphology of N-HOPG at low nitrogen content region

Figure S6 shows Raman spectra of each N-HOPG (X = 0.1, 0.2, 0.3, 0.6, and 2.3). The spectra were normalized according to peak height at 1585 cm^{-1}. The D-band increased with the nitrogen content. The D-band and PDOS-like background were found to gradually broaden and increase, respectively, over X = 0.6.
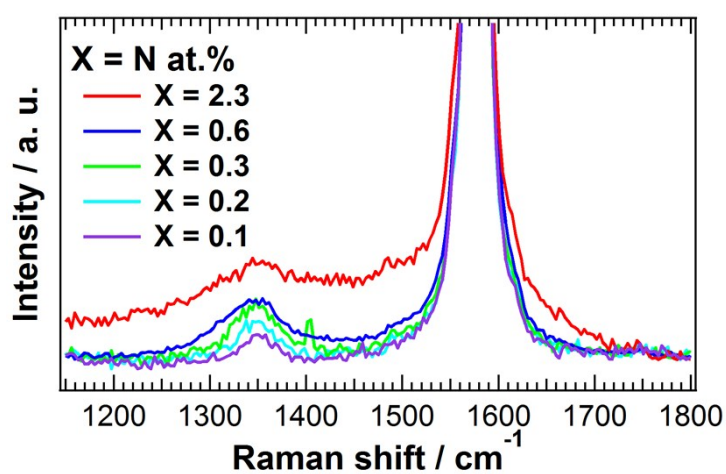

Fig. S6. Raman spectra of each N-HOPG (X = 0.1, 0.2, 0.3, 0.6, and 2.3).

Electrochemical properties of N-HOPG

Figure S7 shows ORR activity of each N-HOPG (X = 0.4, 2.3, and 8.4) and clean HOPG in a 0.1 M H_2SO_4 electrolyte solution. The ORR current was determined by subtracting the N_2 data from the O_2 data.
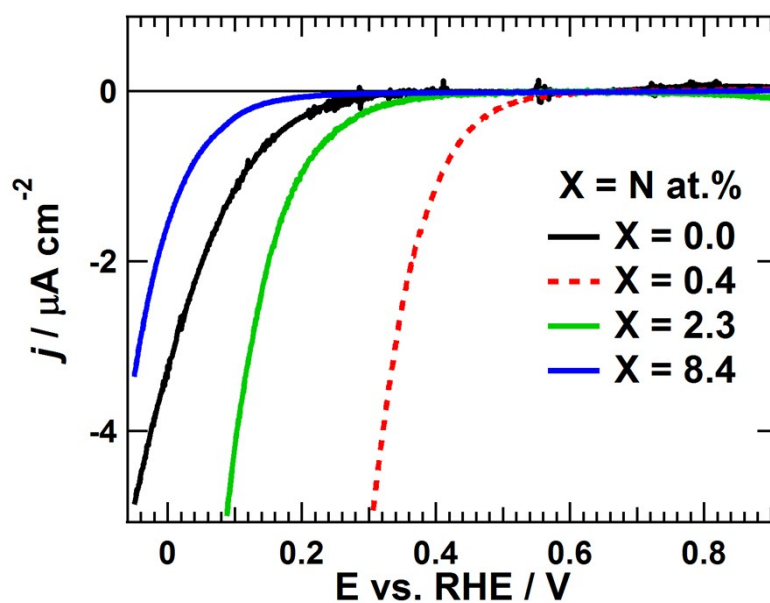

Fig. S7. LSV spectra of each N-HOPG (X = 0.4, 2.3 and 8.4) and clean HOPG (X = 0.0).

References

1. J. F. Ziegler, M. D. Ziegler, and J. P. Biersack, *Nucl. Instruments Methods Phys. Res. Sect. B*, 2010, **268**, 1818–1823.

2. M. Risch and M. Bradley, *Phys. Status Solidi (C)*, 2008, **5**, 939–942.

3. S. E. O'Donnell and P. Reinke, *J. Vac. Sci. Technol. B*, 2009, **27**, 2209–2216.

4. Q. Yang, T. Li, B. King, and R. MacDonald, *Phys. Rev. B*, 1996, **53**, 3032–3038.

5. Y. Senba, S. Yamamoto, H. Ohashi, I. Matsuda, M. Fujisawa, a. Harasawa, T. Okuda, S. Takahashi, N. Nariyama, T. Matsushita, T. Ohata, Y. Furukawa, T. Tanaka, K. Takeshita, S. Goto, H. Kitamura, a. Kakizaki, and M. Oshima, *Nucl. Instruments Methods Phys. Res. Sect. A*, 2011, **649**, 58–60.

6. J. Stöhr, *NEXAFS Spectroscopy*, Springer, 1992.